

High-density holographic data storage with random encoded reference beam

Vladimir B. Markov

MetroLaser, Inc.

18010 Skypark Circle, Suite 100

Irvine CA 92614

vmarkov@metrolaserinc.com

tel: +1-949-553-0688

fax: +1-949-553-0495

Abstract

Holographic technique offers high-density data storage with parallel access and high throughput. Several methods exist for data multiplexing based on the fundamental principle of volume hologram Bragg selectivity. We recently demonstrated that spatial shift selectivity associated with a random (amplitude-phase) encoding of the reference beam is an alternative method for high-density, high capacity data multiplexing. In this report we show some characteristics of the random encoded reference beam hologram selectivity¹.

1 Introduction

Volume holographic memory allows for high throughput data storage and retrieval. Different techniques for data multiplexing have been explored, including those based on angular [2] and spectral [3] selectivity of volume holography, spatial encoding of the reference beam [4] or a combination of these methods [5]. The combination of reference beam phase encoding with spatial-shift multiplexing was shown to be an efficient approach for high-density holographic information storage [6,7]. The correlation effects at volume hologram recording and reconstruction with random encoded (speckled) reference beam came out as the part of the analysis of the holographic laser beam corrector [8]. A similar technique using a reference beam comprised of many plane waves (or a spherical wave) was suggested and experimentally demonstrated [9]. In this report some characteristics of volume hologram with random-encoded reference (RER) beam are discussed.

2 Theoretical Analysis

In our analysis we consider a volume hologram recorded by a plane wave signal beam $S_o(\mathbf{r})$ and a RER-beam, $R_o(\mathbf{r})$, with a divergence $\delta\theta_{SP}$. By intersecting at an angle θ_o these two beams form a hologram with average grating spacing $\Lambda = \lambda/\sin(\theta_o)$, assuming an incidence angle $\theta_{R_o} = 0$. In the first Born approximation, the diffracted beam amplitude $S(\mathbf{r})$, when reconstructed with RER-beam different from the recording one i.e. $R(\mathbf{r}) \neq R_o(\mathbf{r})$, can be described as [10]:

$$S(\mathbf{r}) = k_o^2 \iiint_V \delta\epsilon(\mathbf{r}') R(\mathbf{r}') \frac{\exp[ik_o(\mathbf{r} - \mathbf{r}')] }{4\pi|\mathbf{r} - \mathbf{r}'|} d^3r'. \quad (1)$$

Here $\delta\epsilon(\mathbf{r}) \propto S_o(\mathbf{r})R_o^*(\mathbf{r})$ is the recording media permittivity modulation and V is the volume of the hologram with thickness T . Eq. (1) is valid if $T \gg \lambda/(\delta\theta_{SP})^2$, i.e. exceeds the longitudinal speckle size.

We introduce now the normalized diffracted beam intensity $I_{DN}(\Delta)$ as the parameter to describe the selectivity properties of RER-beam hologram:

$$I_{DN}(\Delta_{\perp}) = \frac{I_D(\Delta_{\perp})}{I_{D(\Delta_{\perp}=0)}} = \frac{\int_0^T \exp\left[\frac{ik_o n \Delta_{\perp}^2}{2d_{dh}}\right] \int_{-\infty}^{+\infty} |P_D(\bar{q})|^2 \times \exp\left[-\frac{ik_o n \bar{q} \Delta_{\perp}}{d_{dh}}\right] d^2 q dz}{T^2 \times \int_{-\infty}^{+\infty} |P_D(\bar{q})|^2 d^2 q} \quad (2)$$

Here the measured diffracted beam intensity $I_D(\Delta)$ is normalized by its peak value at zero shift $I_{D(\Delta=0)}$.

It follows from Eqn. (2) that any spatial mismatch between the hologram and reconstructing beam $\mathbf{R}(\mathbf{r})$ should result in a decline of the diffracted beam intensity. Figure 1 shows the fall-off in $I_{DN}(\Delta_{\perp})$ that occurs for lateral shift Δ_{\perp} . This figure for comparison includes also dependence $I_{DN}(\Delta_{\perp})$ if calculated from a standard correlation function $I_{COR}(\Delta_{\perp})$ from the statistical analysis of the speckle pattern. Comparison of these two curves clearly illustrates the impact of the spatial (volume) interaction on shift selectivity of the RER-beam hologram.

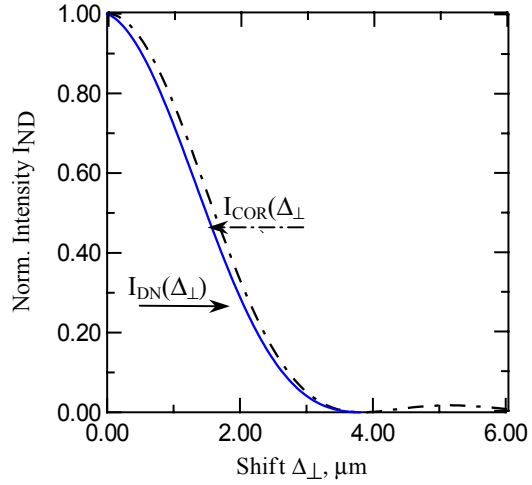


Figure 1. Diffraction beam intensity $I_{DN}(\Delta)$ as a function of lateral Δ_{\perp} shift.

3 Experimental Study

For experimental verification the RER-beam holograms were recorded in 2.3-mm-thick Fe:LiNbO₃ crystal. In a first set of the experiments the crystal was set onto an XY computer controlled positioning table (shift accuracy 0.025 μm in X-Y plane). A 1 cm diameter CW argon laser beam ($\lambda = 515 \text{ nm}$, $P = 40 \text{ mW/cm}^2$) was used as the coherent light source for hologram recording. The laser beam scattered by the ground glass diffuser is then picked up by a large aperture lens ($f\# = 1.4$) forming a subjective speckle pattern in the recording plane. By changing the relative spatial position of the recording scheme elements allows for simple modification of average lateral speckle size $\langle\sigma_{\perp}\rangle$. The RER-beam intersected with the plane wave signal beam at an angle of $\theta_o = 30^\circ$ in air ($\theta_{Ro} = 0^\circ$ and $\theta_{So} = 30^\circ$).

The diffraction efficiency of the hologram in its original position ($\Delta_{\perp} = 0$) was approximately 10^{-3} . After the hologram was recorded, a lateral shift Δ_{\perp} was introduced to evaluate the sensitivity of the reconstruction beam intensity upon lateral shift. A typical example of such operation is shown in Figure 2 for two orthogonal in plane (X-Y) shift direction (a) and for several values of the speckle size $\langle\sigma_{\perp}\rangle$. The solid line in Figure 2 shows the behavior for the angular selectivity that would operate the diffracted beam intensity at identical conditions. Following data from Figure 2 the parameter of shift selectivity can be introduced for RER-beam hologram by analogy with angular selectivity of the plane wave hologram. It is evident also that speckle-shift selectivity has a very smooth character and contrary to the angular Bragg selectivity has no side-lobes in course

of displacement.

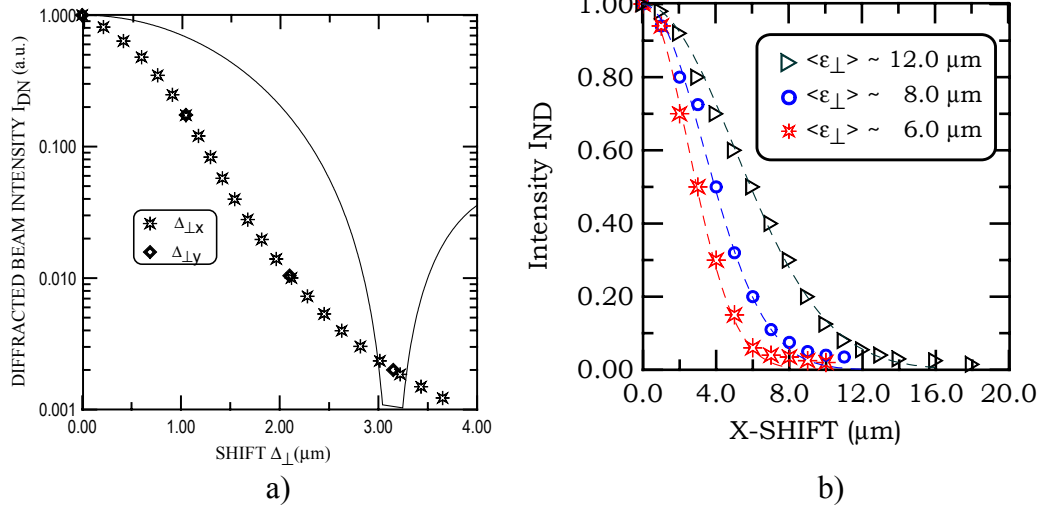


Figure 2. Shift selectivity of RER-hologram (a) and its dependence upon average speckle size $\langle\sigma_{\perp}\rangle$ (b).

3.1 Data recording-retrieval.

To verify experimentally the proposed data storage-retrieval concept, a breadboard system was constructed. A model GSL150/S CW diode-pumped Nd:YAG laser with output power 200 mW at $\lambda = 530 \text{ nm}$ was used as the light source. The SONY model LCX 026AL SLM with window size $2.3 \times 2.3 \text{ mm}$ and pixel size $22.5 \times 22.5 \mu\text{m}$ was used to form a signal channel. The SLM was controlled by a PC that also had a National Instruments PCI-1407 single channel frame grabber for image retrieval. The data retrieval was arranged with the CMOS detector (pixel size $11.0 \times 11.0 \mu\text{m}$).

The detector location and limiting aperture were adjusted to produce the best SLM image onto a CMOS detector array. The pixel pitch of the CMOS detector was $12 \mu\text{m} \times 12 \mu\text{m}$, while that of the SLM was approximately $23 \mu\text{m} \times 23 \mu\text{m}$. The imaging optics was adjusted to produce a magnification of 1 SLM pixel to 2 CMOS pixels. Tests were also conducted using a CCD detector array with a pixel pitch of $8.4 \mu\text{m} \times 9.8 \mu\text{m}$ in place of the CMOS. The magnification in this case was approximately 1 SLM pixel to 2.25 CCD pixels in one axis and 1 SLM pixel to 2.6 CCD pixels in the other.

Once the SLM and detector were properly aligned, tests were conducted in which the data area contained a known, random code and was projected onto either the CMOS or CCD detectors. Each bit of the code was represented by a value of either no attenuation or full attenuation over an area of the SLM. The exact scaling was calculated during each test by the program based on the location of the four dark corners generated by the SLM for alignment.

To test the reliability of the system using the initial test parameters, a series of known, random codes were written to the SLM and read back by the detector. For each test, the code read by the detector was converted back into a digital value and compared to the original code written to the SLM. Experiments in which several hundred codes were written and read were conducted and the location of bits that contained errors was

tracked. Typical results of the random code generation and optical read-out from the CMOS detector are shown in Figure 3, where both original (a) and retrieved (b) fields are presented.



Figure 3. Original (a) and retrieved (b) data-page.

The system was found to be generally reliable; however, some data bits proved to be considerably more prone to errors than the rest. The system also seems to be extremely sensitive to slight changes in alignment. However, at correct alignment of the optical tract the performed tests with about 10^3 cycles allowed us to get the bit-error rate (BER) no higher than three for the entire field of the detection area.

3.2 RER-beam storage in reflection geometry.

As a part of the recording process optimization, we studied the possibility of data multiplexing using a reflection holography scheme. In this geometry the signal and reference beams are illuminating the recording medium from opposite directions, and in this way the reflection grating is formed. The essential benefit of the reflection geometry over the transmission one is the possibility of building a more compact memory module.

Experimentally study of the reflection mode geometry operation the speckle-encoded hologram was recorded with angle $\theta_R = 165^\circ$ between reference RER-beam and object beam. Average speckle size of RER-beam in this experiment was $\langle \sigma_{\perp} \rangle \approx 7 \mu\text{m}$. As it was in transmission geometry the RER-beam was normal to the front surface of LiNbO_3 crystal, and C-axis (optical axis) of the crystal was normal to its front surface. The object beam had an incident angle 30° , propagating from the opposite direction.

No anomalies in the shift selectivity behavior have been observed in this geometry as compared to the transmission one, and a typically measured dependence of the normalized diffracted beam intensity upon spatial decorrelation between recorded and reconstruction positions of the RER-beam (shift selectivity) is shown in Figure 4. It is worth of noting at this point that the angular selectivity of the plane wave hologram recorded in a similar conditions was $\delta\Theta > 5^\circ$ that should result in extremely low storage density, while RER-beam selectivity provides a very good results.

4. Summary and Conclusion

In summary, the random encoded reference beam holographic recording demonstrates extremely high selectivity and therefore high data storage. This selectivity is based on the effects of spatial volumetric decorrelation between the recording and retrieving reconstruction field. Contrary to angular or spectral selectivity of the volume hologram, the two mechanisms that are traditional used for data multiplexing, the RER-beam holograms can be made free from *sinc*-type intensity modulation at its reconstruction. That should result in a much lower cross talk for this type of multiplexing. We demonstrated that the RER-beam hologram operates equally well in both transmission or reflection geometry. These features makes RER-beam hologram architecture attractive for building compact data storage system with ultra-high density and capacity.

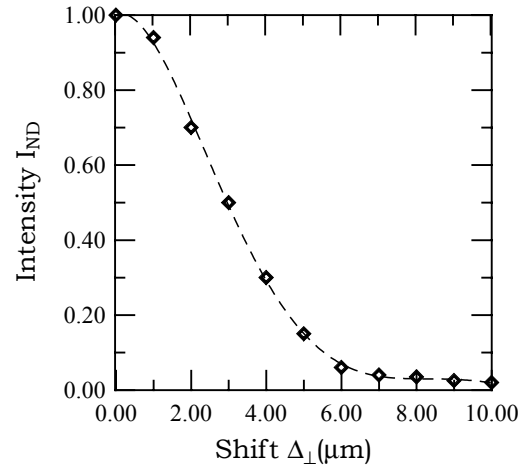


Figure 4. Shift selectivity in reflection geometry

References

- [1] This research was sponsored in part by the US Department of Energy.
- [2] Xin An, D. Psaltis, G. Burr, "Thermal fixing of 10,000 holograms in LiNbO₃:Fe," *Appl. Opt.*, **38**, pp. 386-393 (1999).
- [3] J.Rosen, M. Segev, A. Yariv, "Wavelength-multiplexed computer generated holography", *Opt.Lett.*, **18**, pp.744-746, (1993).
- [4] G. Rakuljic, V. Leyva, A. Yariv, "Optical data storage using orthogonal multiplexed holograms," *Opt.Lett.*, **17**, pp.1471(1992).
- [5] S.Tao, D.Selvian, J.Midwinter, "Spatioangular multiplexed storage of 750 holograms in Fe:LiNbO₃ crystal", *Opt.Lett.*, **18**, pp. 912-914, (1993).
- [6] Darskii, V. Markov, "Information capacity of holograms with a reference speckle-wave grating." *SPIE Proc.* **1600**, 318 (1992).
- [7] V. Markov Yu. Denisyuk, R.Amezquita, "Speckle-shift hologram and its storage capacity", *Opt. Mem. Neural Net.* **6**, 91 (1997).
- [8] V. Markov, M. Soskin, A. Khishnjak, V. Shishkov, Structural conversion of a coherent beam with a volume phase hologram in LiNbO₃" *Soviet Tech. Phys. Lett.*, **4**, pp.304-306, 1978.
- [9] D. Psaltis, M. Leven, A. Pu, G. Barbasthtis, "Holographic storage using shift multiplexing," *Opt. Lett.*, **20**, pp. 782-784, (1995).
- [10] A. Darskii, V. Markov, "Shift selectivity of holograms with reference speckle wave," *Opt. & Spectroscopy*, **65**, pp. 392-395,(1988)

